Novel composite sorbents based on carbon fibers decorated with ferric hydroxides – simultaneous removal of antimonate and arsenate from aqueous solutions

Esra Bilgin Simsek, Pelin Demircivi, Ivan Novak, Dusan Berek and Ulker Beker

ABSTRACT

The competitive adsorption of antimonate and arsenate on carbon fibers decorated with ferric hydroxide (CF-Fe) has been investigated at different pH and temperatures. Tap and drinking water samples spiked with unitary and binary solutions were subjected to kinetic tests and compared with distilled water media. As the required time for attaining the arsenate concentration permitted by law, the legal limit was found as 3 hours for drinking and tap water systems. It was shown that arsenate can be adsorbed more strongly than antimonate. Such multiple adsorption/desorption cycles showed that the CF-Fe sample had approximately 96% of the first antimonate adsorption at the seventh cycle. X-ray photoelectron spectroscopy (XPS) analyses were performed in order to obtain insight into the adsorption mechanism.

Key words | antimony, arsenic, carbon fibers, competitive adsorption, iron oxides

Esra Bilgin Simsek (corresponding author)
Pelin Demircivi
Chemical and Process Engineering Department,
Yalova University,
77100, Yalova, Turkey
E-mail: *esrabilgin622@gmail.com*;
ebilgin.simsek@yalova.edu.tr

Ivan Novak
Dusan Berek
Slovak Academy of Sciences,
Polymer Institute,
84541, Bratislava, Slovakia

Ulker Beker
TÜBITAK Marmara Research Center,
Institute of Chemical Technology,
41470, Gebze, Turkey

INTRODUCTION

Arsenic (As) and antimony (Sb) are toxic and carcinogenic metalloids found in air, soil and natural water and they are found to co-occur in the environment. In geothermal groundwater (Izmir, Turkey), As and Sb concentrations have been reported as 0.7–170 μg/L and 0.06–26 μg/L, respectively (Aksoy *et al.* 2009). In the groundwater near abandoned antimony mines (Slovakia), the levels have been found up to 285 μg/L for As and 1,000 μg/L for Sb (Ungureanu *et al.* 2015). Arsenic and antimony can exist in a variety of oxidation states but they generally occur as Sb(III), Sb(V) and As(III), As(V) in natural aquatic environments (Filella *et al.* 2002; Huang *et al.* 2007). Under oxidized conditions, the dominant forms of As and Sb in aqueous media are arsenate [As(V)] and antimonate [Sb(V)]; while arsenite [As(III)] and antimonite [Sb(III)] are formed under reductive conditions (Lu *et al.* 2015). Antimony is also a bioaccumulative and genotoxic element with similar chemical and toxicological properties to arsenic, and even moderate levels of them can result in harmful environmental effects (Duan *et al.* 2010). Therefore, As and Sb compounds are considered to be priority pollutants by the United States Environmental Protection Agency (US EPA) and the European Union (EU). The EPA, EU and World Health Organization (WHO) have established the maximum contaminant level for arsenic as 10 μg/L in drinking water (WHO 2006; EPA 2012). The maximum contaminant levels of antimony in drinking water were designated as 5 μg/L and 6 μg/L by the EU and US EPA, respectively.

Owing to the legal limits of these metalloids, a significant effort has been made over recent decades to develop effective removal technology to purify water sources. Considering low concentrations of As and Sb in treated

doi: 10.2166/ws.2018.130

water, an adsorption method is advantageous in terms of cost-effectiveness and regeneration capability (Ungureanu *et al.* 2015). Ferric hydroxides exhibit outstanding performance due to their specific chemisorption of As(V) and Sb(V) based on formation of inner-sphere complexes via ligand exchange with OH_2 and/or OH^- groups on the surface (Zhang *et al.* 2014). However, the powder state of these oxides inhibits their widespread use in water treatment owing to the difficulties in separation from water and disposal of the excessive sludge formed during operation. Iron oxide-loaded carbonaceous materials are environmentally benign and exhibit excellent sorption behaviors for numerous contaminants. Recently, among carbonaceous materials, carbon fibers (CF) have been used for remedying various environmental issues due to their special properties like high sorption rate, large surface area, and excellent mechanical stability. They can also serve as a good supporting material for iron oxides (Zhang *et al.* 2010).

Compared with the adsorption studies of arsenic, however, reports on antimony and simultaneous arsenic/antimony removal from water are limited. Moreover, none of the published studies concerning ferric hydroxide-loaded CF refers to the removal of the pentavalent antimony species, which commonly appears in Sb-containing waters. The objective of this work is to examine the effect of partner metalloids on the adsorption and also to achieve the efficient simultaneous removal of As(V) and Sb(V) from aqueous solutions.

MATERIALS AND METHODS

Chemicals and reagents

Sodium arsenate ($Na_2HAsO_4{\cdot}7H_2O$) and potassium hexahydroxyantimonat ($KSb(OH)_6$) were purchased from Sigma-Aldrich. All other chemicals used were of analytical grades.

Preparation of iron-decorated carbon fibers

The microporous CF were prepared according to the procedure described in our previous study (Bilgin Simsek *et al.* 2017). After preparation of raw CF, it was mixed with a solution of $FeCl_3$ (3.0%, wt) and to the slurry was slowly added a solution of 10% NH_4OH until the pH reached the approximate value 10. The suspension was filtered, washed out of all soluble chemicals and dried. The resulting sample was coded as CF-Fe (3%). In order to examine the effect of iron content, CF-Fe (7%), CF-Fe (11%) and CF-Fe (20%) samples were prepared by a similar manner as CF-Fe (3%) with the only difference that the quantity of $FeCl_3$ was 7%, 11% and 20% (wt), respectively.

Adsorption studies

Batch adsorption experiments were conducted by mixing CF or CF-Fe in conical flasks by transferring 25 ml of Sb(V) solution with 100 μg/L Sb(V) concentration at different temperatures (298, 313 and 328 K). The equilibrium As(V) and Sb(V) concentrations were analyzed by an atomic absorption spectrophotometer (Analytik Jena ContrAA 700 TR). Analyses were conducted at a wavelength of 193.7 nm for As and 217.5 nm for Sb using $Pd/Mg(NO_3)_2$ as a matrix modifier.

The effects of pH on Sb(V) adsorption in single and binary systems were studied at different pH levels (3.0–9.0). The solution pH was adjusted and kept constant by using HCl and NaOH. Five milligrams of each sample was added into 25 mL of Sb(V) solution or binary As(V) and Sb(V) solution with an initial concentration of 100 μg/L and a specific pH value.

The kinetic adsorption experiments were performed by mixing single Sb(V) solution or binary As(V) and Sb(V) solution (100 μg/L, pH 5.50 ± 0.2) with CF samples in polyethylene bottles at different temperatures (298, 313, 328 K). The kinetic data were fitted using pseudo-first-order, pseudo-second-order and Weber–Morris diffusion models.

In order to examine the reusability of the carbon fiber adsorbents, desorption and multiple adsorption/desorption cycles were carried out in a batch system. The adsorption tests were conducted by using 0.2 g of adsorbent in a 10 mg/L of Sb(V) solution in a single-component and in a binary system with As(V). The adsorbents were filtrated, washed with distilled water and subjected to desorption tests. Regeneration tests were conducted by stirring the adsorbents in 25 mL NaOH solution (0.5, 1.0 and 3.0 M). Then, the adsorbents were washed with distilled water and dried in an oven prior to re-adsorption tests.

RESULTS AND DISCUSSION

Adsorption experiments

Effect of pH

Variation of the amount of adsorbate as a function of pH can provide information about the nature of the adsorption. In the pH range of 3–5.5, the adsorption capacity of As(V) and Sb(V) for unitary and binary systems increased slightly, whereas it decreased in the pH range of 5.5–9 (Figure 1). CF-Fe (20%) showed high efficiency for both As(V) and Sb(V) when the solution pH was in the range of 5–5.5. As(V) exists in the form of $H_2AsO_4^-$ when the solution pH ranges from 2.1 to 6.7 and in the form of $HAsO_4^{2-}$ when the pH value is higher than 6.7 (Smedley & Kinniburgh 2002). Antimony has mainly two common oxidation states as Sb(III) in anoxic media and Sb(V) in oxic media. The dominant form of Sb(V) for pH values above 4 in water exists as the deprotonated form of antimonic acid, $Sb(OH)_6^-$. Below pH 5, Sb(V) has two coexisting species in water, which are $Sb(OH)_6^-$ and $Sb(OH)_5$. Uncharged antimonous acid, $Sb(OH)_3$, occurs above pH 4 and $Sb(OH)_3$ and $Sb(OH)_2^+$ co-exist below pH 4 as Sb(III) species (Dou *et al.* 2015). The pH_{pzc} values of the samples were found to be in the range of 6.8–8.14. When the solution pH is higher than the pH_{pzc} value, the surface of the CF and CF-Fe is negatively charged. Strong repulsion occurs between the surface and $HAsO_4^{2-}$/$Sb(OH)_6^-$ anions. When the solution pH is lower than pH_{pzc}, electrostatic attractions appear between protonated functional groups ($FeOH_2^+$) and anions. The protonation and deprotonation reactions on the surface according to pH value can be expressed as (Petrova *et al.* 2011):

$$\equiv Fe - OH + H^+ \leftrightarrow FeOH_2^+ \quad pH < pH_{pzc} \tag{1}$$

$$\equiv Fe - OH \leftrightarrow FeO^- + H^+ \quad pH > pH_{pzc} \tag{2}$$

$$\equiv Fe - OH + OH^- \leftrightarrow FeO^- \quad pH > pH_{pzc} \tag{3}$$

Adsorption isotherms

To evaluate the adsorption characteristics of the CF and CF-Fe samples, the isotherm models (Supplementary Material, available with the online version of this paper) were used to analyze adsorption experimental data. Based on the correlation coefficients (R^2) and chi-square (χ^2) values (Table S1), Sb(V) adsorption on both CF and CF-Fe was best described with the Freundlich model, which indicated that Sb(V) is mainly adsorbed in a multilayer coverage manner on active sites with different energy. Besides, it should be noted that the approximate indicator of the adsorption capacity term, K_F, of the Freundlich model is about nine times higher for CF-Fe (20%) than for CF. For the simultaneous adsorption of As(V) and Sb(V), the K_F values also were getting higher as the Fe amount in CF increased. The reason for the enhanced adsorption capacity for higher Fe quantity is the increase in the number of surface functional groups (FeO(O)H) on the adsorbent. Evaluating the results obtained in unitary and binary systems (Figure S1), one can see that adsorption of metalloids in the unitary system was higher than in the binary system. Moreover, it was found that the maximum adsorption capacity was obtained for CF-Fe (20%). In the binary system both metalloids affect each other's adsorption performance (Table S2). It is likely that arsenate takes more available adsorption sites than antimonate both on CF and composite CF-Fe.

Adsorption kinetics

As(V) and Sb(V) adsorption kinetics in unitary and binary systems are presented in Figure 2. For the single-solute As(V) and Sb(V) systems with raw fibers, the equilibrium was reached within 12 and 16 h, respectively. For raw CF, carbonyl and carboxyl groups might play a role in the adsorption (Zhang *et al.* 2010). On the other hand, with CF-Fe (20%) composite the equilibrium was reached within 1 hour for both metalloids. The FeO(O)H groups in the composite structure contain Lewis-acid-type functional groups, and thus, were much more effective for the removal of metalloids when compared with raw CF.

The kinetic data were applied to the pseudo-first-order equation, pseudo-second-order equation and Weber–Morris intra-particle diffusion models (Supplementary Material). As shown in Table S3, for single Sb(V) adsorption, the values of the correlation coefficient of the pseudo-second-order equation were high ($R^2 = 0.99$), confirming the chemical mechanism of the process. The Sb(V) adsorption rate (k_2)

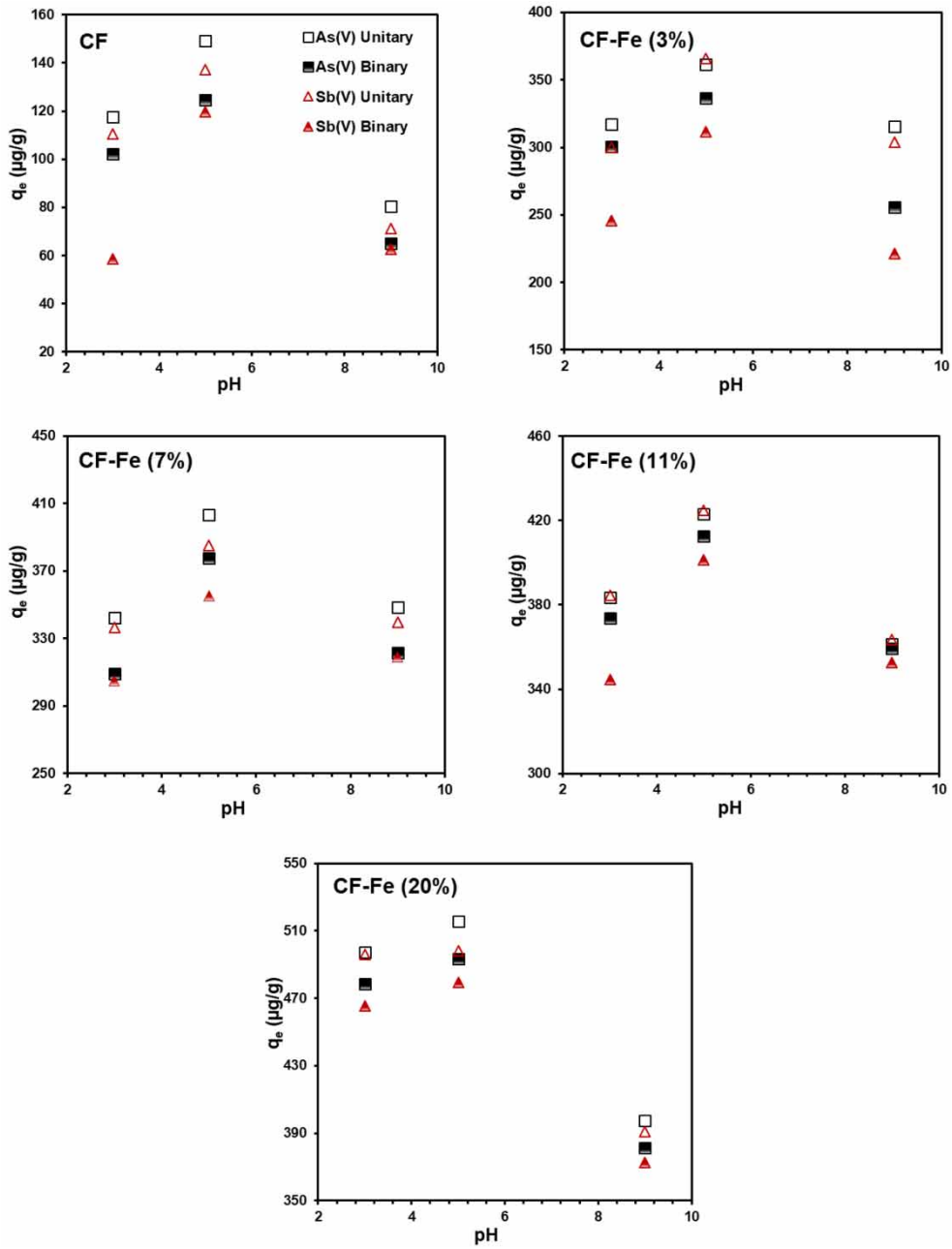

Figure 1 | Effect of pH on As(V) and Sb(V) adsorption in unitary and binary systems.

of CF-Fe (20%) was 2.824×10^{-3} g/µg.min, which is higher than that of CF (0.019×10^{-3} g/µg.min) and indicates that ferric hydroxides on the carbon fiber surface had higher binding affinity to Sb(V).

When two adsorbates compete for adsorption sites, which often occurs in practical situations, the equilibrium requires a longer time. The process of arsenate removal from water was faster than that for antimonate, and 120 min was required to remove 93.8% of As(V) and 86.5% of Sb(V) from the binary solution by the CF-Fe (20%) sample, while 21.5% of As(V) and 11.3% of Sb(V) were removed by CF within 120 min. In the binary system of arsenic and antimony, the uptake of metalloids as a function of time was fitted both with the second-order and

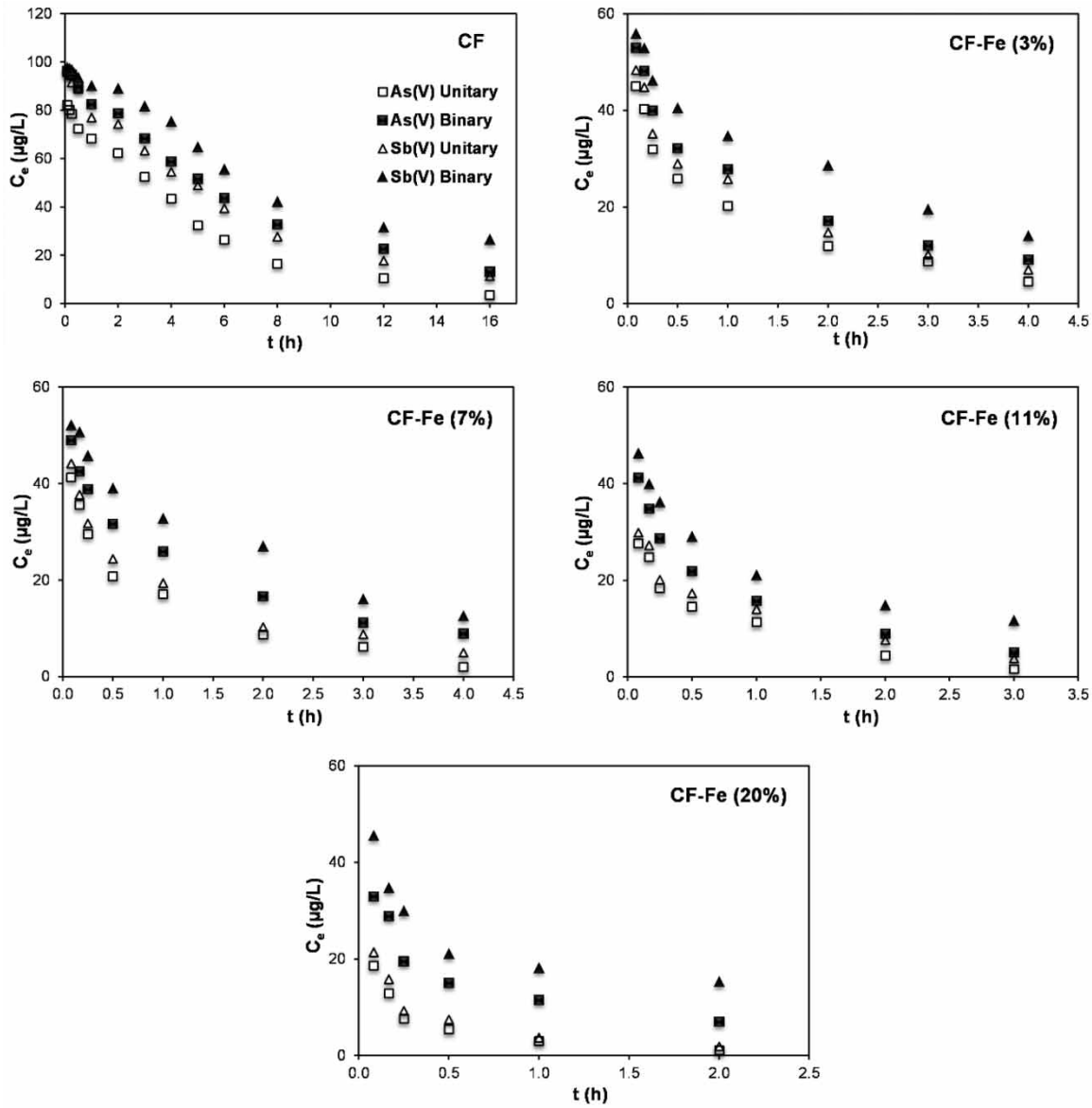

Figure 2 | Adsorption kinetics of As(V) and Sb(V) in unitary and binary systems.

intra-particle diffusion kinetic models (Figure S2). The theoretical adsorption capacities were found to be almost the same as the experimental ones for As(V) and Sb(V) (Table S4). Comparing the unitary system (As or Sb) to the binary (As + Sb) system, for the CF-Fe (3%) sample, the adsorption rate (k_2) of As(V) decreased from 0.655 to 0.427×10^{-3} g/µg.min and k_2 of Sb(V) dropped from 0.489 to 0.372×10^{-3} g/µg.min. Analogous phenomena were observed for other CF-Fe composites.

The Weber–Morris intra-particle diffusion model assumes that sorbate transport within the porous structure of the sorbent is the rate-controlling step of adsorption if the plot of q_t vs $t^{1/2}$ is linear. When the plot is multilinear, it shows that the adsorption is controlled by various limiting factors at different steps of the process. Two straight lines were obtained indicating the external and intra-particle diffusion states (Figure S2(c)). According to the values of the rate parameters (k_{id-1} and k_{id-2}), as well as the correlation

coefficients, the kinetic model indicates that in the first step both arsenic and antimony rapidly equilibrate with the external sites of the adsorbent surface.

Adsorption thermodynamics

Thermodynamic parameters such as Gibbs free energy (ΔG^o), enthalpy change (ΔH^o) and entropy change (ΔS^o) (Supplementary Material, available online) were calculated and the results are given in Table S5. Negative enthalpy changes of CF samples showed the exothermic nature of Sb(V) adsorption in both unitary and binary systems. The positive ΔH^o values of the CF-Fe composites supported the endothermic nature of the adsorption; besides ΔH^o values increased with increasing iron oxide ratio for both unitary and binary systems. The positive ΔS^o values indicate the affinity of samples for As(V) and Sb(V) and the increasing randomness at the solid/liquid interface during adsorption. ΔG^o values of all the samples were found negative, which confirm spontaneous reaction for both unitary and binary systems.

Impact of different water matrices on the adsorption rate

As tap water consists of various types of salts and organic matter, it is a more complex matrix than deionized water and drinking water. Therefore, tap and drinking water samples spiked with both unitary and binary As(V)/Sb(V) solutions were subjected to kinetic adsorption tests and compared with distilled water. The characteristics of tap and drinking water samples are given in Table S6.

The residual arsenic concentration in the unitary system decreased below 10 µg/L after 15 min, 30 min and 2 hours of contact with CF-Fe samples in distilled, drinking and tap water matrices, respectively (Figure 3). These results demonstrate that CF-Fe is an effective adsorbent for arsenic removal in drinking and tap water matrices. On the other hand, the required time to reduce Sb(V) below the allowed level was found to be 1 hour and 2 hours in distilled and drinking water systems, respectively. However, after 3 hours of treatment in the tap water matrix, the equilibrium

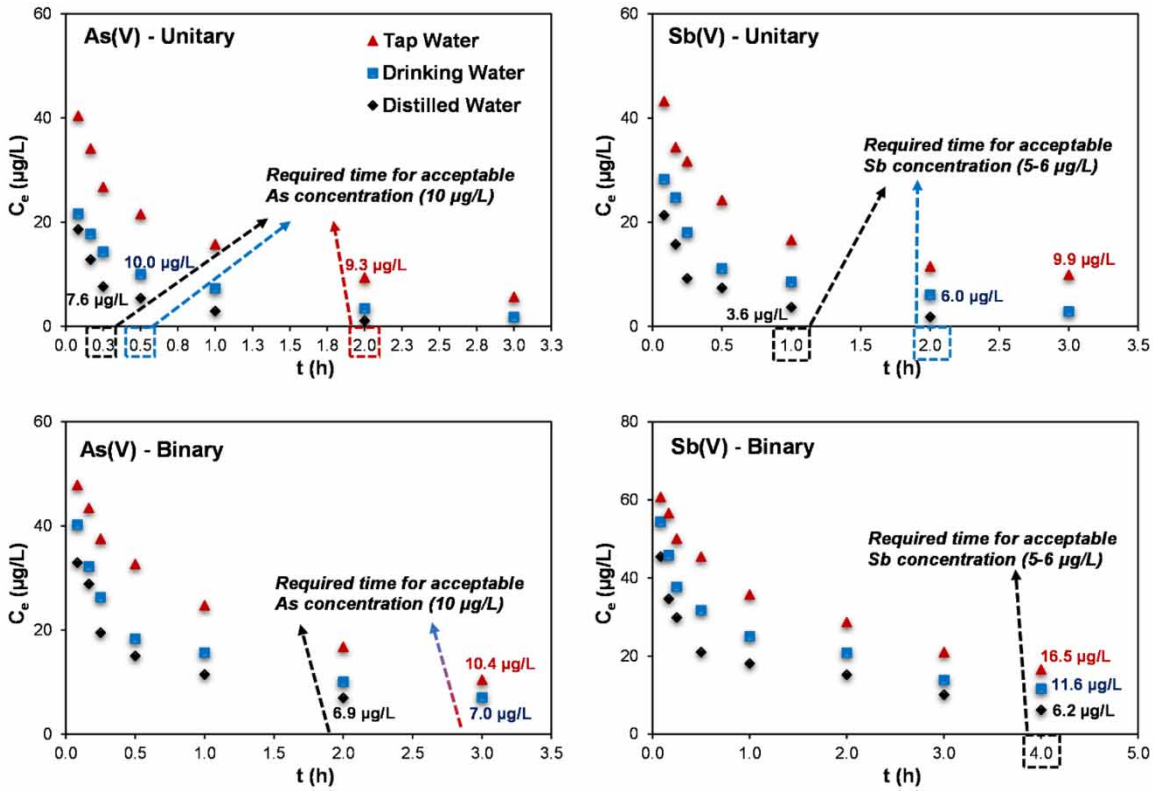

Figure 3 | Adsorption kinetics of As(V) and Sb(V) on CF-Fe (20%) in different water systems.

Sb(V) concentration was found to be 9.9 μg/L, which was above the acceptable level. It can be concluded that the co-existing anions in tap water had a stronger inhibitory effect on Sb(V) removal.

After 120 min of contact with the adsorbent in the binary system, the residual As(V) concentrations were found to be 6.9 μg/L in distilled water, 10.0 μg/L in drinking water and 16.7 μg/L in the tap water matrices. The required time to reach the allowed As(V) concentration was found to be 3 hours for both drinking and tap water. Meanwhile, after 4 hours of treatment, the level of Sb(V) in the binary system was still higher than the maximum allowed contaminant level. The more efficient arsenic and antimony removal from distilled water than from tap water is mainly attributed to the impact of co-existing anions such as sulfate and phosphate in the water.

Micro-characterization XPS analysis for understanding the adsorption mechanism

In order to obtain insight into the arsenate and antimonate adsorption on the CFs, the chemical composition of raw and composite samples after As(V) and Sb(V) adsorption was measured by X-ray photoelectron spectroscopy (XPS) analysis. The O 1s peak of CF-Fe (20%) can be deconvoluted into six peaks (Figure S3(a)). The peaks at 530.6, 531.5 and 532 eV correspond to oxide oxygen (O_2^-), hydroxyl groups (OH^-) and O–C bonds, respectively. After Sb(V) adsorption from the single-solute system onto both CF and CF-Fe (20%) sorbent, the peaks at the binding energy of 530.0 eV appeared with higher proportion attributed to the Sb $3d_{5/2}$ core level (Luo *et al.* 2015). In the spectra of As(V) and Sb(V) adsorbed CFs, the intensities of the band at 532.5 eV increased due to the formation of O–As chemical states. Moreover, new bands appeared at 533 eV, which can be ascribed to the presence of H_2O on the saturated surface. Owing to their similar chemical nature, arsenic and antimony share similar sorption behavior. It can be concluded that both metalloids were mainly adsorbed through the hydroxyl groups (OH^-) via surface complexation by forming inner-sphere complexes.

The high resolution C 1s spectra of CF (Figure S3(b)) could be curve-fitted into six peak components with binding energies assigned of 284.3, 286.4, 288.8, 284.9, 283.7 and 285.5 eV attributable to C–C, C–O, O–C–O (or COOH), C = C, C = O and C–H, respectively (Singh *et al.* 2014; Kumar & Jiang 2016). After adsorption, the ratio of oxygen-bonded C states decreased, suggesting that the surface functional groups including oxygen are involved in the unitary or binary adsorption.

The As 3d spectra of the saturated CFs (Figure S3(c)) in unitary and binary systems exhibited similar characteristic As(V) peaks, in one band centered at approximately 45.0 eV. Unlike the unitary system, in addition to the As(V) peak, new peaks of the Sb 4d core level at 36.0 eV appeared in the spectra of binary system indicating that Sb(V) were also adsorbed onto the CFs.

Desorption and stability experiments

Desorption and recycling experiments were conducted to examine the stability of the CF and CF-Fe (20%) samples (Figure S4). The single Sb(V) desorption efficiencies of CF were found to be 63.4%, 83.1%, and 92.4% when 0.5, 1.0 and 3.0 M NaOH were used as agents, while the desorption efficiencies for the CF-Fe (20%) sample were found to be 73.7%, 84.6% and 96.6%, respectively. By using NaOH solution as desorption agent, arsenate or antimonate are desorbed with the Donnan exclusion effect (Jais *et al.* 2016).

After selecting the optimum desorption agent (3.0 M NaOH), the cycle was repeated seven times (Figure S4). In the first cycle, for the CF and CF-Fe (20%) samples, Sb(V) desorption efficiencies (in the unitary system) were found to be 92.4% and 96.6%, while they decreased to 88.9% and 76.5% after the seventh cycle, respectively. In addition, CF and CF-Fe (20%) had approximately 82% and 96% of the first antimonate adsorption capacity at the seventh re-adsorption cycle, showing the reusability of these sorbents.

In contrast to the single-solute system, both desorption efficiency and adsorption capacity decreased much less in the binary system during the cycles. Sb(V) adsorption capacity (in the binary system) decreased to 71.0% and 79.4% for the CF and CF-Fe (20%) samples, respectively. On the other hand, for both the unitary and binary systems, the ferric-hydroxide-decorated carbon fiber sample was found more stable when compared with CF. In the binary system, the As(V) adsorption capacity of CF-Fe (20%) was

80.5% of the initial capacity after seven adsorption–desorption cycles while it was found to be 72.4% for CF.

CONCLUSION

CF decorated with different quantities of ferric hydroxide were synthesized. As(V) and Sb(V) adsorption from both model single and two-component adsorbate was evaluated. It was found that the composite fibers exhibited much higher adsorption efficiency than raw fiber. Increased amounts of ferric hydroxide resulted in higher As(V) and Sb(V) adsorption performance for both unitary and binary systems. The As(V) and Sb(V) adsorption mechanism on CF-Fe was proposed to be electrostatic attraction, hydrogen bonding and inner-sphere complexation dependent on the pH of the medium. The As(V) and Sb(V) levels were found to be below the maximum allowed contaminant level so that the CF-Fe composites can be used as efficient, cost-effective adsorbent for the removal of metalloids from aquatic media. It can be concluded that the ferric-hydroxide-decorated carbon fiber composites can present an alternative to existing commercial adsorbents for the treatment of drinking water.

REFERENCES

Aksoy, N., Şimşek, C. & Gunduz, O. 2009 Groundwater contamination mechanism in a geothermal field: a case study of Balcova, Turkey. *Journal of Contaminant Hydrology* **103** (1–2), 13–28.

Bilgin Simsek, E., Novak, I., Sausa, O. & Berek, D. 2017 Microporous carbon fibers prepared from cellulose as efficient sorbents for removal of chlorinated phenols. *Research on Chemical Intermediates* **43** (1), 503–522.

Dou, X., Mohan, D., Zhao, X. & Pittman Jr, C. H. 2015 Antimonate removal from water using hierarchial macro-/mesoporous amorphous alumina. *Chemical Engineering Journal* **264**, 617–624.

Duan, L. Q., Song, J. M., Li, X. G. & Yuan, H. M. 2010 The behaviors and sources of dissolved arsenic and antimony in Bohai Bay. *Continental Shelf Research* **30**, 1522–1534.

EPA 2012 *2012 Edition of the Drinking Water Standards and Health Advisories*. Office of Water, US Environmental Protection Agency, Washington, DC, USA.

Filella, M., Belzile, N. & Chen, Y. W. 2002 Antimony in the environment: a review focused on natural waters: I. Occurrence. *Earth-Science Reviews* **57**, 125–176.

Huang, C. Z., Hu, B. & Jiang, Z. 2007 Simultaneous speciation of inorganic arsenic and antimony in natural waters by dimercaptosuccinic acid modified mesoporous titanium dioxide micro-column on-line separation and inductively coupled plasma optical emission spectrometry determination. *Spectrochimica Acta Part B* **62**, 454–460.

Jais, F. M., Ibrahim, S., Yoon, Y. & Jang, M. 2016 Enhanced arsenate removal by lanthanum and nano-magnetite composite incorporated palm shell waste-based activated carbon. *Separation and Purification Technology* **169**, 93–102.

Kumar, A. S. K. & Jiang, S. J. 2016 Chitosan-functionalized graphene oxide: a novel adsorbent an efficient adsorption of arsenic from aqueous solution. *Journal of Environmental Chemical Engineering* **4**, 1698–1713.

Lu, H., Zhu, Z., Zhang, H., Zhu, J. & Qiu, Y. 2015 Simultaneous removal of arsenate and antimonate in simulated and practical water samples by adsorption onto Zn/Fe layered double hydroxide. *Chemical Engineering Journal* **276**, 365–375.

Luo, J., Luo, X., Crittenden, J., Qu, J., Bai, Y., Peng, Y. & Li, J. 2015 Removal of antimonite (Sb(III)) and antimonate (Sb(V)) from aqueous solution using carbon nanofibers that are decorated with zirconium oxide (ZrO_2). *Environmental Science and Technology* **49**, 11115–11124.

Petrova, T. M., Fachikov, L. & Hristov, J. 2011 The magnetite as adsorbent for some hazardous species from aqueous solutions: a review. *International Review of Chemical Engineering* **3**, 134–152.

Singh, B., Fang, Y., Cowie, B. C. C. & Thomsen, L. 2014 NEXAFS and XPS characterization of carbon functional groups of fresh and aged biochars. *Organic Geochemistry* **77**, 1–10.

Smedley, P. L. & Kinniburgh, D. G. 2002 A review of the source, behaviour and distribution of arsenic in natural waters. *Applied Geochemistry* **17**, 517–568.

Ungureanu, G., Santos, S., Boaventura, R. & Botelho, C. 2015 Review: arsenic and antimony in water and wastewater: overview of removal techniques with special reference to latest advances in adsorption. *Journal of Environmental Management* **151**, 326–342.

WHO 2006 *Guidelines for Drinking-Water Quality: First Addendum to Volume 1, Recommendations*, 3rd edn. World Health Organization, Geneva, Switzerland.

Zhang, S., Li, X. Y. & Chen, J. P. 2010 An XPS study for mechanisms of arsenate adsorption onto a magnetite-doped activated carbon fiber. *Journal of Colloid and Interface Science* **343**, 232–238.

Zhang, H., Li, L. & Zhou, S. 2014 Kinetic modeling of antimony(V) adsorption–desorption and transport in soils. *Chemosphere* **111**, 434–440.

First received 14 February 2018; accepted in revised form 24 June 2018. Available online 9 July 2018